CHEMICAL REACTION, HEAT AND MASS TRANSFER EFFECTS ON MHD PERISTALTIC TRANSPORT IN A VERTICAL CHANNEL THROUGH SPACE POROSITY AND WALL PROPERTIES

D. Chenna Kesavaiah[1], M. Karuna Prasad[2], G. Bhaskar Reddy[3], Dr. Nookala Venu[4]

[1]Department of Basic Sciences & Humanities, Vignan Institute of Technology and Science, Deshmukhi (V), Pochampally (M), Yadadri-Bhuvanagiri (Dist), T.S-508284, India
Email: chennakesavaiah@gmail.com

[2]Department of Mathematics, GITAM School of Science, GITAM (Deemed to be University), Bengaluru, Karanata, Pin -562163, India
Email: dprasadm@gitam.edu

[3]Department of Science and Humanities, A M Reddy Memorial College of Engineering & Technology, Petlurivaripalem (V), Narasaraopet, Andhra Pradesh-522601, India
Email: drgbhaskarreddy@gmail.com

[4]Department of Electronics and Communication Engineering,
Balaji Institute of Technology and Science (Autonomous), Narsampet, Warangal, TS -506331, India
Email: venunookala@gmail.com

ABSTRACT

The present paper analyzed on magnetohydrodynamic peristaltic transport flow of a Newtonian fluid through porous space in a vertical channel with compliant walls under the assumptions of long wavelength and low Reynolds number with chemical reaction, heat and mass transfer. The governing partial differential equations derived and solved by using perturbation method. The physical behaviour of different parameters for velocity, temperature and concentration profiles has been examined through graphically and the phenomenon of trapping has been discussed.

Keywords: Peristalsis, Porous space, Hartmann number, Schmidt number, Chemical reaction

DOI Number: 10.14704/nq.2022.20.11.NQ66076 **NeuroQuantology 2022; 20(11): 781-794**

INTRODUCTION

The study of peristalsis has received considerable attention in the last four decades manly because of its potential application to the biological systems. It is a mechanism for fluid transport which is achieved by the passage of progressive waves of area contraction and expansion over flexible walls of a tube containing fluid. The word peristalsis stems from the Greek word ‘peristaltikos’ which means clasping and compressing. It consisting narrowing and transverse shortening of apportion of a tube, which then relaxes, while a lower portion becomes shortened and narrowed. Some worms like earth-worm use peristalsis for their locomotion. Form fluid mechanical point of view peristaltic pumping is characterized by the dynamical interaction of fluid flow with movement of flexible boundaries. Peristalsis appears to be the major mechanism for urine transport of spermatozoa in the ducts efferentes of the male reproductive organs, movement of egg in female fallopian tubes, motion of spermatozoa in cervical canal and transport of bile in bile duct. It has been suggested that peristalsis may be associated with the vasomotion of small blood vessels. In view of above some of the authors carried out their research work, (Wang et al, 2008) studied by long wavelength approximation to peristaltic flow of an Oldroyd 4-constant fluid in a planar channel, (Chenna Kesavaiah et al, 2021) explained in detail of radiative MHD Walter's Liquid-B flow past a semi-infinite vertical plate in the presence of viscous dissipation with a heat source, (Ali Nasir and Hayat Tasawar, 2007) expressed their view on peristaltic motion of a Carreau fluid in an asymmetric channel, (Rami Reddy et al, 2021) has been considered Hall Effect on MHD flow of a viscoelastic fluid through porous medium over an infinite vertical porous plate with heat source, (Chenna Kesavaiah and Venkateswarlu, 2020) shows that chemical reaction and radiation absorption effects on convective flows past a porous vertical wavy channel with travelling thermal waves, (Elshehawey and Husseny, 2000) depicted the effects of porous boundaries on peristaltic transport through a porous medium, (Mallikarjuna Reddy et al, 2019) observed on radiation and diffusion thermo effects of viscoelastic fluid past a porous surface in the presence of magnetic field and chemical reaction with heat source, Heat transfer to MHD free convection flow of a viscoelastic dusty gas through a porous medium with chemical reaction studied by (Srinathuni Lavanya and Chenna Kesavaiah, 2017), (Ch Kesavaiah et al, 2013) depicted the effects of radiation and free convection currents on unsteady Couette flow between two vertical parallel plates with constant heat flux and heat source through porous medium, (Yeddala et al, 2016) intended the finite difference solution for an MHD Free Convective rotating flow past an accelerated vertical plate.

A peristaltic pump is a device for transporting fluids usually from a region of lower pressure to higher pressure by means of a contraction wave propagating along a tube like structure. This traveling wave phenomenon is termed as peristalsis. In fact peristalsis originated from the pumping of physiological fluids in a living body. Most of the physiological systems such as ureter, bile duct, stomach and blood vessels are reported to follow the mechanism of peristalsis pumping fluid may be a single fluid or a mixture of more than one fluid, while pumping physiological fluids from one place to another. In several physiological functions, which contains the blood flow through vessels are exaggerated by the frequency of drug uses. In various serious circumstances such as tightening by the body muscles, excretion of many materials changes due to diverse biochemical reactions. The blood flow rate through vessels arteries is also be exaggerated due to drug pedestrian. The injured body portions can be only revamped by using drugs, on the other hand, their reinstatement is not possible. Many of the clinician's reflections show that drug have sophisticated effectiveness may be less operational because the drug has many side effects. (Mallikarjuna Reddy et al, 2018) motivated study on effects of radiation and thermal diffusion on MHD heat transfer flow of a dusty viscoelastic fluid between two moving parallel plates. (Chenna Kesavaiah and Sudhakaraiah, 2014) extended the effects of heat and mass flux to MHD flow in vertical surface with radiation absorption. (Maryiam Javed et al, 2014) has been considered peristaltic flow of Burgers fluid with compliant wall and heat transfer, (Reese et al, 1997) explained A model of a combined porous peristaltic pumping system, in Physiological fluid Dynamics II, Proc. 2^{nd} International Conference on Physiological fluid dynamics, Chenna Kesavaiah et. al. (2013) expressed on natural convection heat transfer oscillatory flow of an elastico-viscous fluid from vertical plate, (Ellahi, 2013) has been studied the effects of MHD and temperature dependent viscosity on the flow of non-Newtonian nanofluid in a pipe: analytical solutions, (Chenna Kesavaiah and Satyanarayana, 2013) has done motivated study on MHD and Diffusion Thermo effects on flow accelerated vertical plate with chemical reaction, (Rajaiah and Sudhakaraiah, 2015) carried out the research work on unsteady MHD free convection flow past an accelerated vertical plate with chemical reaction and Ohmic heating, (Haranth and Sudhakaraiah, 2015) has been studied viscosity and Soret effects on unsteady hydromagnetic gas flow along an inclined plane, (Chenna Kesavaiah et al, 2013) considered the radiation and Thermo - Diffusion effects on mixed convective heat and mass transfer flow of a viscous dissipated fluid over a vertical surface in the presence of chemical reaction with heat source, (Karunakar Reddy et al, 2013) shows that MHD heat and mass transfer flow of a viscoelastic fluid past an impulsively started infinite vertical plate with chemical reaction.

The physical mechanism of the flow induced by the traveling wave can be well understood and is known as the so-called peristaltic transport mechanism. Peristaltic pumping is also used in medical instruments such as the heart-lung machine. Investigation on peristaltic transport of non-Newtonian fluid is of utmost importance owing to its wide range of applications in engineering and biology which have smooth muscle tubes such as lower intestine, gastrointestinal tract, cervical canal, female fallopian tube, lymphatic vessels and small blood vessels. In particular, the study of such fluids has applications in a number of processes that occur in industry such as the extrusion of polymer fluids, solidification of liquid crystals, cooling of metallic plate in a bath, exotic lubricants, colloidal and suspension solutions. Further, such analysis may serve for the intrauterine fluid motion in a sagittal cross section of the uterus under cancer therapy and drug analysis. Also, peristaltic transport occurs in many practical applications involving biomechanical systems such as roller and finger pumps. In the past, several theoretical and experimental investigations have been made to understand peristalsis in different situations. (Rajaiah and Sudhakaraiah, 2015) illustrated the radiation and Soret effect on Unsteady MHD flow past a parabolic started vertical plate in the presence of chemical reaction with magnetic dissipation through a porous medium,0 (Ch Kesavaiah et al 2012) explained in detail on radiation and mass transfer effects on moving vertical plate with variable temperature and viscous dissipation, (Satyanarayana et al, 2011) expressed the viscous dissipation and thermal radiation effects on an unsteady MHD convection flow past a semi-infinite vertical permeable moving porous plate, (Ch Kesavaiah et al, 2011) shows that the effects of the chemical reaction and radiation absorption on an unsteady MHD convective heat and mass transfer flow past a semi-infinite vertical permeable moving plate embedded in a porous medium with heat source and suction, (Brasseur et al, 1987) shows that the influence of a peripheral layer of different viscosity on peristaltic pumping with Newtonian fluids, (Shapiro et al, 1969) depicted peristaltic pumping with long wave length at low Reynolds number, (Elshehawey et al, 2000) illustrated Peristaltic transport in a cylindrical tube through a porous medium, (Hayat et al, 2008) motivated study on MHD peristaltic transport of a Jeffery fluid in a channel with compliant walls and porous space, (Hou et al, 1989) carried out their research work on boundary conditions at the cartilage – Synovival fluid interface for joint lubrication and theoretical verification, (Mittra and Prasad, 1973) On the influence of wall properties and Poiseuille flow in peristalsis, (Ramachandra Rao and Usha, 1995) motivated study on peristaltic pumping in a circular tube in the presence of an eccentric catheter, (Shukla et al, 1980) illustrated the effects of peripheral layer viscosity on peristaltic transport of a bio-fluid, (Chenna Kesavaiah et al, 2021) has been studied MHD effect on convective flow of dusty viscous fluid with fraction in a porous medium and heat generation, (Hayat and Hina, 2010) expressed their views on the influence of wall properties on the MHD peristaltic flow of a Maxwell fluid with heat and mass transfer, (Radhakrishnamacharya and Srinivasulu, 2007) considered the influence of wall properties on peristaltic transport with heat transfer, (Mekheimer et al, 2009) shown that the effects of heat transfer and space porosity on peristaltic flow in a vertical asymmetric channel.

The main goal of the present study is to investigate the heat and mass transfer effects on MHD peristaltic flow in a vertical porous space with compliant walls in the presence of chemical reaction taking into an account. The features of flow characteristics are analyzed by plotting graphs. The organization of the paper is as follows. The problem is formulated includes the solution of the problem under the long wavelength and low-Reynolds number assumptions. Numerical results and discussions are presented with help of graphs. Also the conclusions have been summarized in detailed.

FORMULATION OF THE PROBLEM

We consider the motion of an incompressible viscous fluid through a porous medium in a vertical two-dimensional symmetric channel induced by sinusoidal wave trains propagating with constant speed c along the walls. A constant magnetic field of strength B_0 is applied across the channel. A coordinate system is chosen such that the x-axis is parallel to the gravitational acceleration vector g, but in the opposite direction. The y-axis is orthogonal to the channel walls, and the origin of the axes is such that the positions of the channel walls are $y=-\eta$ and $y=\eta$, respectively. The wall $y=-\eta$ at is at the given uniform temperature $T=T_1'$ while the wall at $y=\eta$ is subjected to a uniform temperature T_2', where $T_2'>T_1'$. In addition, the concentration of a certain constituent in the solution varies from C_1' on the inner surface of the left wall to C_2' on the inner surface of the right wall. The geometry of the channel wall is given by

$$y=\eta(x,t)=d+a\sin\frac{2\pi}{\lambda}(x-ct) \qquad (1)$$

and the equations governing the motion for the present problem are

$$\frac{\partial u}{\partial x}+\frac{\partial v}{\partial y}=0 \qquad (2)$$

$$\begin{aligned}\rho\left(\frac{\partial u}{\partial t}+u\frac{\partial u}{\partial x}+v\frac{\partial u}{\partial y}\right)&=-\frac{\partial p}{\partial x}\\ &+\mu\left(\frac{\partial^2 u}{\partial x^2}+\frac{\partial^2 u}{\partial y^2}\right)-\frac{\mu\varphi}{k}u-\sigma B_0^2 u \quad (3)\\ &+\rho g_t\,\beta(T-T_1')+\rho g\beta_c(C-C_1')\end{aligned}$$

$$\begin{aligned}\rho\left(\frac{\partial v}{\partial t}+u\frac{\partial v}{\partial x}+v\frac{\partial v}{\partial y}\right)&=-\frac{\partial p}{\partial y}\\ &+\mu\left(\frac{\partial^2 v}{\partial x^2}+\frac{\partial^2 v}{\partial y^2}\right)-\frac{\mu\varphi}{k}v \end{aligned} \qquad (4)$$

$$\rho C_p\left(\frac{\partial T}{\partial t}+u\frac{\partial T}{\partial x}+v\frac{\partial T}{\partial y}\right)=\frac{K}{\rho}\left(\frac{\partial^2 T}{\partial x^2}+\frac{\partial^2 T}{\partial y^2}\right)+\mu\left\{2\left(\frac{\partial u}{\partial x}\right)^2+\left(\frac{\partial v}{\partial y}\right)^2+\left(\frac{\partial u}{\partial x}+\frac{\partial v}{\partial y}\right)^2\right\} \quad (5)$$

$$\left(\frac{\partial C}{\partial t}+u\frac{\partial C}{\partial x}+v\frac{\partial C}{\partial y}\right)=D_m\left(\frac{\partial^2 C}{\partial x^2}+\frac{\partial^2 C}{\partial y^2}\right)-K_r'\left(C-C_1'\right) \quad (6)$$

The boundary conditions Radhakrishnamacharya and Srinivasulu [35]

$$u=0 \quad at \ y=\pm\left[d+a\sin\frac{2\pi}{\lambda}(x-ct)\right] \quad at \ y=\mp\eta \quad (7)$$

$$\frac{\partial}{\partial x}L(\eta)=\frac{\partial p}{\partial x}=\mu\left(\frac{\partial^2 u}{\partial x^2}+\frac{\partial^2 u}{\partial y^2}\right)-\rho\left(\frac{\partial u}{\partial t}+u\frac{\partial u}{\partial x}+v\frac{\partial u}{\partial y}\right)-\frac{\mu\varphi}{k}u \quad (8)$$
$$-\sigma B_0^2 u+\rho g\beta_t(T-T_1')+\rho g\beta_c(C-C_1')$$

$$T=T_1' \qquad C=C_1' \quad on \quad y=-\eta \quad (9)$$

$$T=T_2' \qquad C=C_2' \quad on \quad y=\eta \quad (10)$$

B_0 is transverse magnetic field, D_m is coefficient of mass diffusivity, p is pressure, T is temperature, k is permeability of the medium, k_T is thermal-diffusion ratio T_1' and T_2' is wall temperatures, C_1' and C_2' are wall concentrations, $\overline{T}$ is mean value of T_1' and T_2', λ is non-dimensional wave number, ω is frequency parameter, ρ is density, β_t is coefficient of thermal expansion, β_c is coefficient of expansion with concentration, φ is the porosity of the medium, ψ is stream function, ν is kinematic viscosity, and σ is coefficient of electric conductivity.

$L=-\tau\frac{\partial^2}{\partial x^2}+m\frac{\partial^2}{\partial t^2}+C^*\frac{\partial}{\partial t}$. Here τ is the elastic tension in the membrane, m is the mass per unit area and C^* is the coefficient of viscous damping.

Introducing such that $u=-\frac{\partial\psi}{\partial y}$ and $v=\frac{\partial\psi}{\partial x}$ and the following non-dimensional quantities

$$x'=\frac{x}{d},\qquad y'=\frac{y}{d},\qquad \psi'=\frac{\psi}{cd}$$
$$t'=\frac{ct}{d}\qquad \theta=\frac{T-T_1'}{T_2'-T_1'} \quad (11)$$
$$\phi=\frac{C-C_1'}{C_2'-C_1'},\ \eta'=\frac{\eta}{d},\ p'=\frac{pd^2}{c^2\lambda\mu}$$

in equations (1)-(10) , we finally get (after dropping primes)

$$R\delta\left[\frac{\partial^2\psi}{\partial x^2\partial t}+\frac{\partial\psi}{\partial y}\frac{\partial^2\psi}{\partial x\partial y}-\frac{\partial\psi}{\partial x}\frac{\partial^2\psi}{\partial y^2}\right]=-\frac{\partial p}{\partial x}+\delta^2\left(\frac{\partial^3\psi}{\partial x^2\partial y}+\frac{\partial^3\psi}{\partial y^3}\right)-H^2\frac{\partial\psi}{\partial y}-G_t(\theta+N\phi) \quad (12)$$

$$R\delta^3\left[\frac{\partial^2\psi}{\partial x^2\partial t}+\frac{\partial\psi}{\partial y}\frac{\partial^2\psi}{\partial x^2}-\frac{\partial\psi}{\partial x}\frac{\partial^2\psi}{\partial y\partial x}\right]=-\frac{\partial p}{\partial x}+\delta^2\left(\delta^2\frac{\partial^3\psi}{\partial x^3}+\frac{\partial^3\psi}{\partial x\partial y^2}\right)-\sigma^2\delta^2\frac{\partial\psi}{\partial y} \quad (13)$$

$$R\Pr\delta\left[\frac{\partial\theta}{\partial t}-\frac{\partial\psi}{\partial y}\frac{\partial\theta}{\partial x}-\frac{\partial\psi}{\partial x}\frac{\partial\theta}{\partial y}\right]=\left(\delta^2\frac{\partial^2\theta}{\partial x^2}+\frac{\partial^2\theta}{\partial y^2}\right)+B_r\left\{4\delta^2\left(\frac{\partial^2\psi}{\partial x\partial y}\right)^2+\left(\frac{\partial^2\psi}{\partial y^2}-\delta^2\frac{\partial^2\psi}{\partial x^2}\right)^2\right\} \quad (14)$$

$$R\delta\left[\frac{\partial\phi}{\partial t}+\frac{\partial\psi}{\partial y}\frac{\partial\phi}{\partial x}-\frac{\partial\psi}{\partial x}\frac{\partial\phi}{\partial y}\right]= \frac{1}{Sc}\left(\delta^2\frac{\partial^2\phi}{\partial x^2}+\frac{\partial^2\phi}{\partial y^2}\right)-Kr\phi \quad (15)$$

$$\delta^2\left(\frac{\partial^3\psi}{\partial x^2\partial y}+\frac{\partial^3\psi}{\partial y^3}\right)- R\delta\left[\frac{\partial^2\psi}{\partial x^2\partial t}+\frac{\partial\psi}{\partial y}\frac{\partial^2\psi}{\partial x\partial y}-\frac{\partial\psi}{\partial x}\frac{\partial^2\psi}{\partial y^2}\right] -H^2\frac{\partial\psi}{\partial y}-G_t\left(\theta+N\phi\right) =\left[E_1\frac{\partial^3}{\partial x^3}+E_2\frac{\partial^3}{\partial t^2\partial x}+E_3\frac{\partial^2}{\partial t\partial x}\right]\eta \quad (16)$$

$$\frac{\partial\psi}{\partial y}=0 \quad at \ y=\pm\eta =\pm\left[1+\varepsilon\sin\frac{2\pi}{\lambda}(x-ct)\right] \quad (17)$$

$$\theta=0 \qquad \phi=0 \quad on \qquad y=-\eta \quad (18)$$

$$\theta=1 \qquad \phi=1 \quad on \qquad y=\eta \quad (19)$$

where

$H^2,\varepsilon,\delta,R,M,\sigma^2,\Pr,Ec,B_r,G_t,N,Sc,Kr$ geometric parameters, Reynolds number, Hartmann number, porosity parameter are E_1,E_2,E_3 are the non-dimensional elasticity parameters, Prandtl number, Eckert number, Brinkmann number, Grashof number and chemical reaction

$$H^2=\sigma^2+M^2,\ \varepsilon=\frac{a}{d},\delta=\frac{d}{\lambda},\ R=\frac{cd\rho}{\mu}$$

$$M^2=\frac{\sigma}{\mu}B_0d,\quad \sigma^2=\frac{\varphi d^2}{k},\qquad Br=Ec\Pr$$

$$E_1=-\frac{\tau d^3}{\lambda\mu c},\ E_2=\frac{mcd^3}{\lambda^3\mu},\qquad E_3=\frac{C^*d^3}{\lambda^2\mu}$$

$$Ec=\frac{c^2}{c_p\left(T_2'-T_1'\right)},\Pr=\frac{\mu C_p}{K},Sc=\frac{\mu}{\rho D_m}$$

$$E_1=-\frac{\tau d^3}{\lambda\mu c},\quad E_2=\frac{mcd^3}{\lambda^3\mu},\quad E_3=\frac{C^*d^3}{\lambda^2\mu}$$

$$Ec=\frac{c^2}{c_p\left(T_2'-T_1'\right)},\qquad N=\frac{\beta_c\left(C_2'-C_1'\right)}{\beta_t\left(T_2'-T_1'\right)}$$

$$Kr=\frac{Kr'd^2}{c},\qquad G_t=\frac{\rho g\beta_t\left(T_2'-T_1'\right)d^2}{\mu c}$$

METHOD OF SOLUTION

Using the long wavelength approximation and neglecting the wave number along with low-Reynolds number, one can find from Equations (12) to (16) that

$$0=-\frac{\partial p}{\partial x}+\frac{\partial^2\psi}{\partial y^3}-H^2\frac{\partial\psi}{\partial y}+G_t\left(\theta+N\phi\right) \quad (20)$$

$$0=-\frac{\partial p}{\partial y} \quad (21)$$

Equation (21) shows that p is not function of y.

$$0=\frac{\partial^2\theta}{\partial y^2}-B_r\left(\frac{\partial^2\theta}{\partial y^2}\right)^2 \quad (22)$$

$$0=\frac{1}{Sc}\frac{\partial^2\phi}{\partial y^2}-Kr\phi \quad (23)$$

$$\frac{\partial^3\psi}{\partial y^3}-H^2\frac{\partial\psi}{\partial y}-G_t\left(\theta+N\phi\right)=\left[E_1\frac{\partial^3}{\partial x^3}+E_2\frac{\partial^3}{\partial t^2\partial x}+E_3\frac{\partial^2}{\partial t\partial x}\right]\eta \qquad (24)$$

It is not possible to get closed form solutions for Equations (20) and (22)-(23) for arbitrary values of all the parameters. We seek perturbation solutions in terms of the Grashof number G_t, porosity parameter σ^2 and Hartmann number M^2 as follows Mekheimer et al. [36]

$$f=\left(f_{00}+G_t f_{01}+..........\right)+H^2\left(f_{10}+G_t f_{11}+.........\right)+..... \qquad (25)$$

where f is any flow variable, substituting (25) in the equations (18)-(20) and (22)-(24), and collecting the coefficients of various powers of G_t and H^2, we get the following sets of equations:

Zeroth order:

$$0=-\frac{\partial p_{00}}{\partial x}+\frac{\partial^3\psi_{00}}{\partial y^3} \qquad (26)$$

$$0=\frac{\partial^2\theta_{00}}{\partial y^2}+B_r\left(\frac{\partial^2\psi_{00}}{\partial y^2}\right)^2 \qquad (27)$$

$$0=\frac{1}{Sc}\frac{\partial^2\phi_{00}}{\partial y^2}-Kr\phi_{00} \qquad (28)$$

with boundary conditions:

$$\frac{\partial\psi_{00}}{\partial y}=0 \quad at \quad y=\pm\eta \qquad (29)$$

$$\theta_{00}=0,\phi_{00}=0 \quad on \quad y=-\eta \qquad (30)$$

$$\theta_{00}=1,\phi_{00}=1 \quad on \quad y=\eta \qquad (31)$$

$$\frac{\partial^3\psi_{00}}{\partial y^3}=\frac{\partial p_{00}}{\partial x}=\left\{E_1\frac{\partial^3\eta}{\partial x^3}+E_2\frac{\partial^3\eta}{\partial t^2\partial x}+E_3\frac{\partial^2\eta}{\partial t\partial x}\right\} \qquad (32)$$

First order:

$$0=-\frac{\partial^3\psi_0}{\partial y^3}+\left(\theta_{00}+N\phi_{00}\right) \qquad (33)$$

$$0=\frac{\partial^2\theta_{01}}{\partial y^2}+2B_r\left(\frac{\partial^2\psi_{00}}{\partial y^2}\frac{\partial^2\psi_{01}}{\partial y^2}\right) \qquad (34)$$

$$0=\frac{1}{Sc}\frac{\partial^2\phi_{01}}{\partial y^2}-Kr\phi_{01} \qquad (35)$$

and

$$0=\frac{\partial^3\psi_{10}}{\partial y^3}-\frac{\partial\psi_{00}}{\partial y} \qquad (36)$$

$$0=\frac{\partial^2\theta_{10}}{\partial y^2}+2B_r\left(\frac{\partial^2\psi_{00}}{\partial y^2}\frac{\partial^2\psi_{10}}{\partial y^2}\right) \qquad (37)$$

$$0=\frac{1}{Sc}\frac{\partial^2\phi_{10}}{\partial y^2}-Kr\phi_{10} \qquad (38)$$

with conditions:

$$\frac{\partial\psi_{01}}{\partial y}=0,\theta_{01}=0,\phi_{01}=0 \quad at \quad y=\pm\eta \qquad (39)$$

$$\frac{\partial\psi_{10}}{\partial y}=0,\theta_{10}=0,\phi_{10}=0 \quad at \quad y=\pm\eta \qquad (40)$$

Solving the above sets of equations, we get

$$\psi_{00}=8\varepsilon\pi^3\left\{\frac{E_3}{2\pi}\sin 2\pi\left(x-t\right)-\left(E_1+E_2\right)\cos 2\pi\left(x-t\right)\right\}\left(\frac{y^3}{6}-\frac{\eta^2 y}{2}\right)$$

$$\theta_{00} = \frac{1}{2}\left(1+\frac{y}{\eta}\right)+\frac{16\varepsilon^2\pi^6}{3}\left\{\frac{E_3}{2\pi}\sin 2\pi(x-t) -(E_1+E_2)\cos 2\pi(x-t)\right\}^2\left(\eta^4-y^4\right)$$

$$\phi_{00} = Z_1 e^{m_1 y} + Z_2 e^{m_2 y}$$

$$\psi_{01} = A_1\left(\frac{y^3}{6}-\frac{\eta^2}{2}\right)+A_2\left(\frac{y^4}{24}-\frac{\eta^2 y^2}{12}\right) + A_3\left(\frac{y^7}{210}-\frac{\eta^6 y}{30}\right)$$

$$\theta_{01} = \frac{B_1}{6}\left(y^3-\eta^2 y\right)+\frac{B_2}{12}\left(y^4-\eta^4\right) + \frac{B_3}{20}\left(y^5-\eta^5 y\right)+\frac{B_4}{56}\left(y^8-\eta^8\right)$$

$$\phi_{01} = 0$$

$$\psi_{10} = \frac{L}{2}\left(\frac{y^5}{60}-\frac{\eta^4 y}{12}\right)-\frac{L\eta^2}{2}\left(\frac{y^3}{6}-\frac{\eta^2 y}{2}\right)$$

$$\theta_{10} = \frac{B_5}{12}\left(y^4-\eta^4\right)+\frac{B_6}{30}\left(y^6-\eta^6\right)$$

$$\phi_{10} = 0$$

RESULTS AND DISCUSSIONS

To study the behaviour of solutions, numerical calculations for several values of porosity parameter $\left(\sigma^2\right)$, Hartmann number (M), Brinkman number (Br), Grashof number (G_t), buoyancy ratio parameter (N), Schmidt number (Sc), Chemical reaction parameter (Kr) , occlusion parameter, the elastic tension i.e., the rigidity of the wall (E_1), the mass characterizing parameter i.e., the stiffness of the wall (E_2) and damping nature of the wall (E_3) have been carried out. Figure (1) shows the influence of M, σ^2, G_t, Sc, N, E_1, E_2 and E_3 on velocity distribution with fixed values of $E_1 = 1.0, E_2 = 0.5, E_3 = 0.5, Kr = 1.0,$ $Br = 1.0, N = 1.0, \quad \varepsilon = 0.2, t = 0.1, x = 0.2$. The effect of different values of M on velocity is graphed in Figure 1(a). It is interesting to note that the effect of increasing Hartmann number leads to a decrease in the velocity throughout the channel. This is because of the presence of the transverse magnetic field which creates a resistive force similar to the drag force that acts in the opposite direction of the fluid motion, thus causing the velocity of the fluid to decrease. Figure 1(b) has been plotted to depict the variation of velocity for different values of porosity parameter. From this graph we observe that velocity decreases with an increase of porosity parameter. Figure 1(c) illustrates the effect of the Grashof number on the velocity field. It is found that the effect of increasing Grashof number is to increase the velocity as expected. An increase in the Grashof number physically means an increase of the buoyancy force, which supports the flow. Figure 1 (d) depicts the graph of velocity profiles for various values of Sc. We observe from this graph that increasing Sc leads to a decrease in the velocity. Figure 1(e) represents graph of velocity distribution for different values of buoyancy ratio parameter N. It is observed that increasing N suppresses the velocity. The influence of wall membrane parameters (E_1, E_2) on the velocity field is presented in Figure 1(f). It shows that velocity enhances with increasing E_1, E_2. Figure 1(g) show that effect of E_3. It is observed that the velocity decreases with an increase of E_3. To see the effects of $Br, \varepsilon, G_t, N, S, E_1, E_2$ and E_3 on temperature distribution, we have plotted Figure (2). The effect of increasing *r B* on the temperature distribution is plotted in Figure 2 (a). One can observe that the temperature increases with increasing Br. Further, it is observed that that the temperature profiles are almost parabolic except when $Br=0$. A similar result can be noticed in Figure 2 (b) if Br is replaced by ε. Figure 2 (c) has been plotted to see the variation of temperature profiles against y for different values of G_t. By analyzing the graphs it reveals that temperature increases with an increase of G_t. The effect of changing N on θ is presented in Figure 2 (d). It can easily be seen that Kr is increased by increasing N but there is no appreciable difference. Figure 2 (e) is the graph of θ for different values of Kr. It is observed that increasing Kr leads to decreases in the fluid temperature. Figure 2 (f) is a plot of temperature profile for changing E_1, E_2 with constant values of other parameters. It displays that temperature enhances as E_1, E_2 increases. Figure 2(g) is plot of temperature profiles for changing E_3 it decreases with an increase of E_3. The influence of the parameters of Sc, Kr on concentration distribution is graphed in Figure (3). Figure 3 (a) is plotted for $Kr = 1.0, 2.0, 3.0, 4.0$. It is observed that with increasing in Kr the concentration decreases. Figure 3 (b) is plotted for $Sc =$ 0.5, 0.6, 0.78, 1, 2 (which corresponds to Hydrogen gas, water vapour, ammonia, carbon dioxide at $25^\circ C$, Ethyl benzene in air) on concentration. It shows that increasing Sc reduces the fluid concentration.

CONCLUSION

The following results observed after the study of this paper:

- The effects of various emerging parameters on flow, heat and mass transfer characteristic have been studied. It is observed that increasing G_t, E_1, E_2 leads to increasing fluid velocity whereas a reverse trend is seen with increasing M, σ^2, Sc and E_3.
- The temperature profiles are almost parabolic and the temperature increases with an increase of $G_t, E_1, E_2, \varepsilon$ N while it decreases with increasing Kr and E_3. Further, the trapped bolus decreases in size with increasing Hartmann number. Also, we can note that the trapped bolus have mixed behaviour (i.e. it decreases for $x<0.2$ and increases for $x>0.2$) with increasing N.
- The results of hydrodynamics case for non-porous space can be captured as a limiting case of our analysis by taking M and $\sigma^2 \to 0$.

APPENDIX

$$L = 8\varepsilon\pi^3 \left[\begin{array}{l} \dfrac{E_3}{2\pi}\sin 2\pi(x-t) \\ -(E_1+E_2)\cos 2\pi(x-t) \end{array} \right]$$

$$A_1 = \frac{1}{2}(1-N) + \frac{BrL^2\eta^4}{12}(1-NScKr)$$

$$A_2 = \frac{1}{2\eta}(1-N),\ \ A_3 = \frac{BrL^2}{12}(1-NScKr)$$

$$B_1 = \frac{B_r A_2}{3}, B_2 = -2B_r A_1 L$$

$$B_3 = -2B_r A_2 L, B_4 = \frac{2B_r A_3 L}{5}$$

$$B_5 = \frac{L^2}{6}, B_6 = \frac{L^2\eta^2}{2} + 2B_r$$

$$Z_1 = -\frac{e^{-m_2}}{2\sinh(m_2-m_1)}$$

$$Z_2 = -\frac{e^{-m_1}}{2\sinh(m_1-m_2)}$$

REFERENCES

Wang Y, Hayat T and Oberlack M. Long wavelength approximation to peristaltic flow of an Oldroyd 4-constant fluid in a planar channel, Biorheology, 2008; 45: 611-628

Chenna Kesavaiah Damala, Venkateswarlu Bhumarapu, Oluwole Daniel Makinde. Radiative MHD Walter's Liquid-B flow past a semi-infinite vertical plate in the presence of viscous dissipation with a heat source, Engineering Transactions, 2021; 69 (4): 373–401

Ali Nasir and Hayat Tasawar. Peristaltic motion of a Carreau fluid in an asymmetric channel, Applied Mathematics and Computation, 2007; 193: 535-552

Rami Reddy G, Chenna Kesavaiah D, Venkata Ramana Musala and Bkaskara Reddy G. Hall Effect on MHD flow of a viscoelastic fluid through porous medium over an infinite vertical porous plate with heat source, Indian Journal of Natural Sciences, 2021; 12 (68): 34975-34987

Chenna Kesavaiah D and Venkateswarlu B. Chemical reaction and radiation absorption effects on convective flows past a porous vertical wavy channel with travelling thermal waves, International Journal of Fluid Mechanics Research, 2020; 47 (2): 153-169

Elshehawey E F and Husseny S Z A. Effects of porous boundaries on peristaltic transport through a porous medium, Acta Mechnica, 2000; 143: 165-177.

Mallikarjuna Reddy B, D Chenna Kesavaiah D and Ramana Reddy G V. Radiation and diffusion thermo effects of viscoelastic fluid past a porous surface in the presence of magnetic field and chemical reaction with heat source, Asian Journal of Applied Sciences, 2019; 7 (5): 597-607

Srinathuni Lavanya and Chenna Kesavaiah D. Heat transfer to MHD free convection flow of a viscoelastic dusty gas through a porous medium with chemical reaction, International Journal of Pure and Applied Researches, 2017; 3 (1): 43 - 56

Mallikarjuna Reddy B, Chenna Kesavaiah D and Ramana Reddy G. Effects of radiation and thermal diffusion on MHD heat transfer flow of a dusty viscoelastic fluid between two moving parallel plates, ARPN Journal of Engineering and Applied Sciences, 2018; 13 (22): 8863-8872

Chenna Kesavaiah D and Sudhakaraiah A. Effects of heat and mass flux to MHD flow in vertical surface with radiation absorption, Scholars Journal of Engineering and Technology, 2014; 2(2): 219-225

Maryiam Javed, Hayat T and Alsaej A. Peristaltic flow of Burgers fluid with compliant wall and heat transfer, Applied Mathematics and Computation, 2014; 244: 654-671

Reese G W and Rath H J. A Model of a combined porous peristaltic pumping system, in Physiological fluid Dynamics II, Proc. 2nd International Conference on Physiological fluid dynamics, IIT Madras, L.S. Srinath and M. Singh, Eds, Tata McGraw-Hill, New Delhi, 1997; 190-195.

Chenna Kesavaiah D, P V Satyanarayana P V, Sudhakaraiah A, Venkataramana S. Natural convection heat transfer oscillatory flow of an elastico-viscous fluid from vertical plate, International Journal of Research in Engineering and Technology, 2013; 2 (6): 959-966

Ellahi R. The effects of MHD and temperature dependent viscosity on the flow of non-Newtonian nanofluid in a pipe: Analytical solutions, Appl. Math. Model., 2013; 37: 1451-1467

Chenna Kesavaiah D and Satyanarayana P V. MHD and Diffusion Thermo effects on flow accelerated vertical plate with chemical reaction, Indian Journal of Applied Research, 2013; 3 (7): 310-314

Rajaiah M and Sudhakaraiah A. Unsteady MHD free convection flow past an accelerated vertical plate with chemical reaction and Ohmic heating, International Journal of Science and Research, 2015; 4 (2): 1503-1510

Haranth Y and Sudhakaraiah A. Viscosity and Soret effects on Unsteady Hydromagnetic gas flow along an inclined plane, International Journal of Science and Research, 2015; 4 (2): 2650-2654

Chenna Kesavaiah D, Satyanarayana P V and Venkataramana S. Radiation and Thermo - Diffusion effects on mixed convective heat and mass transfer flow of a viscous dissipated fluid over a vertical surface in the presence of chemical reaction with heat source, International Journal of Scientific Engineering and Technology, 2013; 2 (2): 56-72

Karunakar Reddy S, Chenna Kesavaiah D and Raja Shekar M N. MHD heat and mass transfer flow of a viscoelastic fluid past an impulsively started infinite vertical plate with chemical reaction, International Journal of Innovative Research in Science, Engineering and Technology, 2013; 2 (4): 973- 981

Rajaiah M and Sudhakaraiah. Radiation and Soret effect on Unsteady MHD flow past a parabolic started vertical plate in the presence of chemical reaction with magnetic dissipation through a porous medium, International Journal of Science and Research, 2015; 4 (2): 1608-1613

Ch Kesavaiah D, Satyanarayana P V and A Sudhakaraiah A. Effects of radiation and free convection currents on unsteady Couette flow between two vertical parallel plates with constant heat flux and heat source through porous medium, International Journal of Engineering Research, 2013; 2 (2): 113-118

Yeddala H, Sudhakaraiah A, Venkatalakshmi P and Sivaiah M. Finite difference solution for an MHD free convective rotating flow past an accelerated vertical plate, i-manager's Journal on Mathematics, 2016; 5 (2): 34-44

Ch Kesavaiah D, Satyanarayana P V, Gireesh Kumar J and Venkataramana S. Radiation and mass transfer effects on moving vertical plate with variable temperature and viscous dissipation, International Journal of Mathematical Archive, 2012; 3 (8): 3028-3035

Satyanarayana P V, Ch Kesavaiah D and Venkataramana S. Viscous dissipation and thermal radiation effects on an unsteady MHD convection flow past a semi-infinite vertical permeable moving porous plate, International Journal of Mathematical Archive, 2011; 2(4): 476-487

Ch Kesavaiah D, P V Satyanarayana P V and Venkataramana S. Effects of the chemical reaction and radiation absorption on an unsteady MHD convective heat and mass transfer flow past a semi-infinite vertical permeable moving plate embedded in a porous medium with heat source and suction, Int. J. of Appl. Math and Mech., 2011; 7 (1): 52-69

Brasseur J G, Corrsin S and Lunan Q. The influence of a peripheral layer of different viscosity on peristaltic pumping with Newtonian fluids, J. Fluid Mech., 1987; 174: 495-519

Shapiro A H, Jaffrin M Y and Weinberg S L. Peristaltic pumping with long wave length at low Reynolds number, J. Fluid Mech., 1969; 37: 799-825

Elshehawey E F and E L Sebaei W (2000). Peristaltic transport in a cylindrical tube through a porous medium, Int. J. Math. Sci., 2000; 24 (4): 217-230

Hayat T, Javad M and Ali N. MHD Peristaltic transport of a Jeffery fluid in a channel with compliant walls and porous space, Transport of porous media, 2008; 74: 259-274.

Hou J S, Holmes M H, Lai W M and Mow V C. Boundary conditions at the cartilage – Synovival fluid interface for joint lubrication and theoretical verification, Trans. ASME J. Biomech. Engg., 1989; 111: 78-87

Mittra T K and Prasad S N. On the influence of wall properties and Poiseuille flow in peristalsis, Journal of Biomechanics, 1973; 6: 681-693

Ramachandra Rao A and Usha S. Peristaltic pumping in a circular tube in the presence of an eccentric catheter, Trans. ASME J. Biochem. Engg, 1995; 117: 448-454.

Shukla J B, Parihar R S, Rao B R P and Gupta S P. Effects of peripheral layer viscosity on peristaltic transport of a bio-fluid, J. Fluid Mech., 1980; 97: 225-237

Chenna Kesavaiah D, Ramakrishna Goud T, Nookala Venu and Seshagiri Rao Y V. MHD effect on convective flow of dusty viscous fluid with fraction in a porous medium and heat generation, Journal of Mathematical Control Science and Applications, 2021; (7) 2: 393-404

Hayat T and Hina S. The influence of wall properties on the MHD peristaltic flow of a Maxwell fluid with heat and mass transfer, Nonlinear Analysis: Real world Applications, 2010; 11 (4): 3155-3169

Radhakrishnamacharya G and Srinivasulu Ch. Influence of wall properties on peristaltic transport with heat transfer, C. R. Mecanique, 2007; 335: 369-373

Mekheimer Kh S, Husseny S Z A and Abd Elmaboud Y. Effects of heat transfer and space porosity on peristaltic flow in a vertical asymmetric channel, Numerical Mathematics for Partial Differential Equations, 2009; 26: 747-770

Chenna Kesavaiah D, Ramakrishna Goud T, Nookala Venu and Seshagiri Rao Y V. MHD effect on convective flow of dusty viscous fluid with fraction in a porous medium and heat generation, Journal of Mathematical Control Science and Applications, 2021; 7 (2): 393-404

Chenna Kesavaiah D, Ramakrishna Goud T and Seshagiri Rao Y V Nookala Venu. Radiation effect to MHD oscillatory flow in a channel filled through a porous medium with heat generation, Journal of Mathematical Control Science and Applications, 2019; 5 (2): 71-80

Chenna Kesavaiah D, Ramakrishna Goud T, Nookala Venu and Seshagiri Rao Y V. Analytical study on induced magnetic field with radiating fluid over a porous vertical plate with heat generation, Journal of Mathematical Control Science and Applications, 2017; 3 (2): 113-126

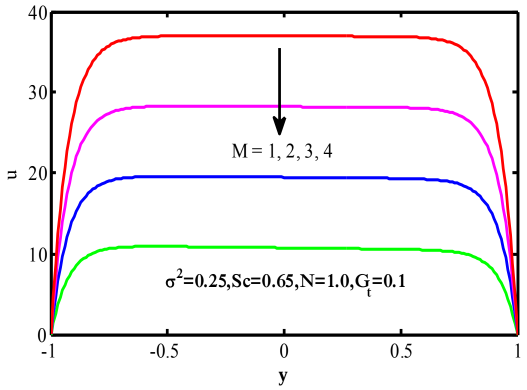

Fig.1 (a): Velocity profile for M

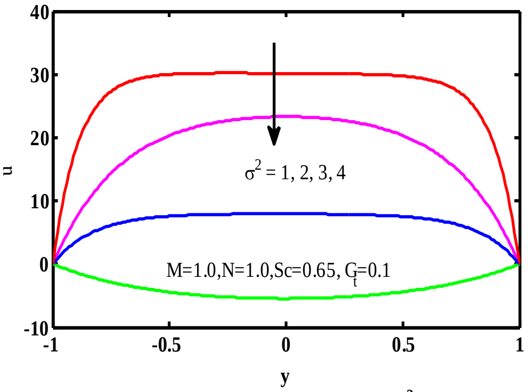

Fig. 1(b): Velocity profiles for σ^2

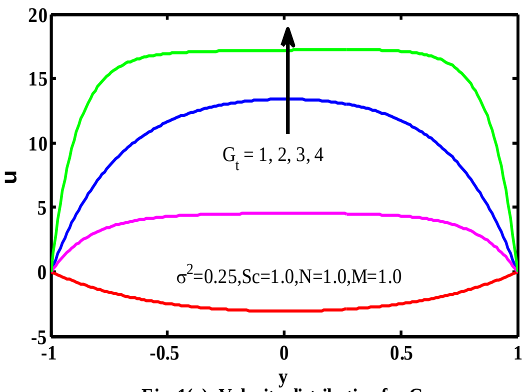

Fig. 1(c): Velocity distribution for G_t

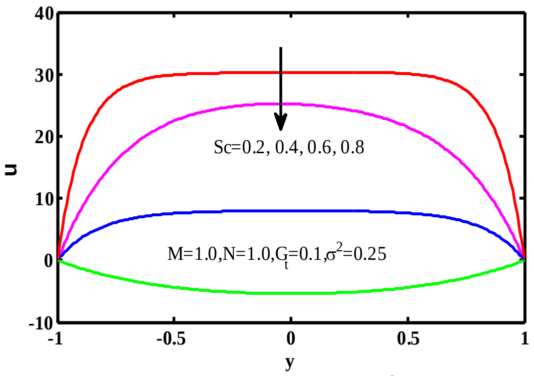

Fig. 1(d): Velocity distribution for Sc

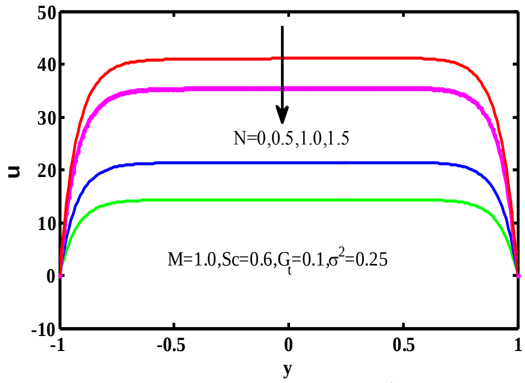

Fig. 1(e): Velocity distribution for N

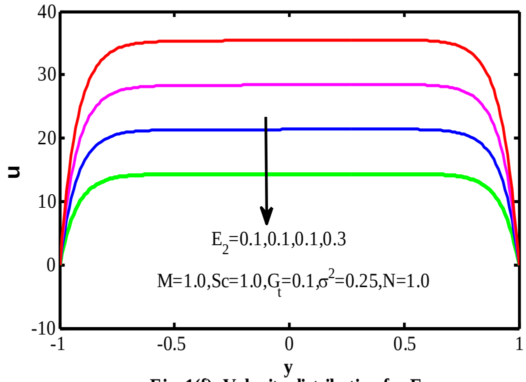

Fig. 1(f): Velocity distribution for E_3

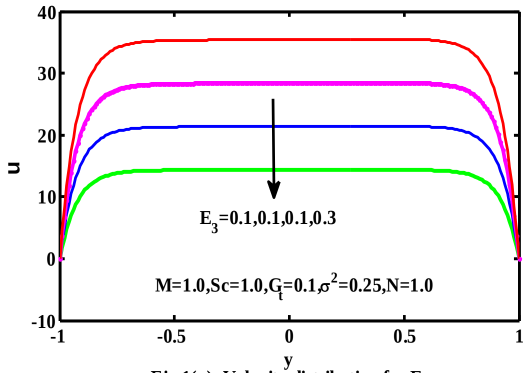

Fig.1(g): Velocity distribution for E_3

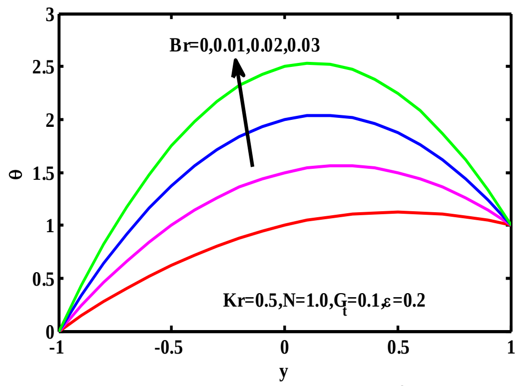

Fig. 2 (a): Temperature distribution for Br

eISSN 1303-5150

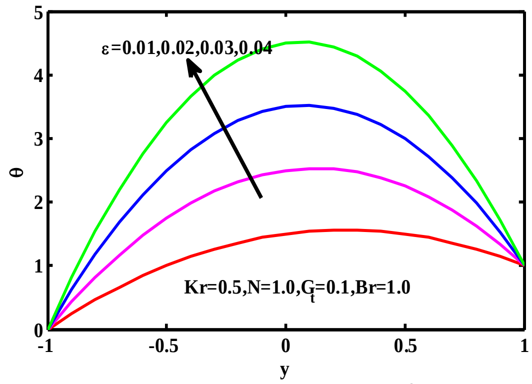

Fig 2(b): Temperature distribution for ε

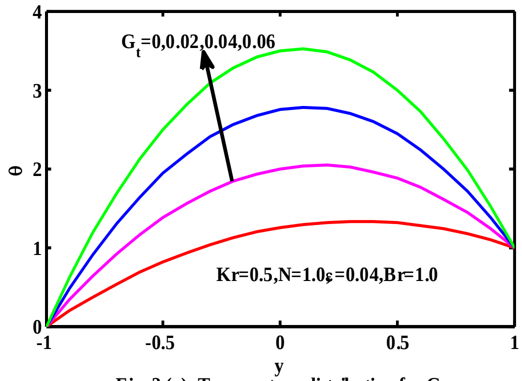

Fig. 2 (c): Temperature distribution for G_t

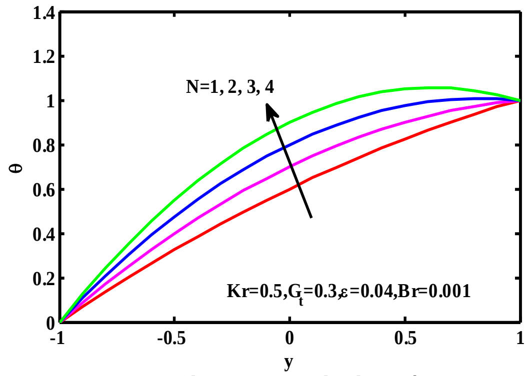

Fig. 2 (d): Temperature distribution for N

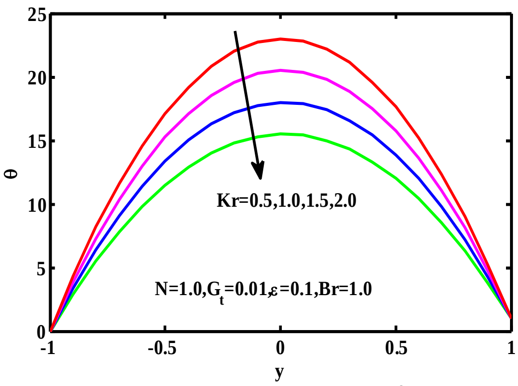

Fig. 2 (e): Temperature distribution for Kr

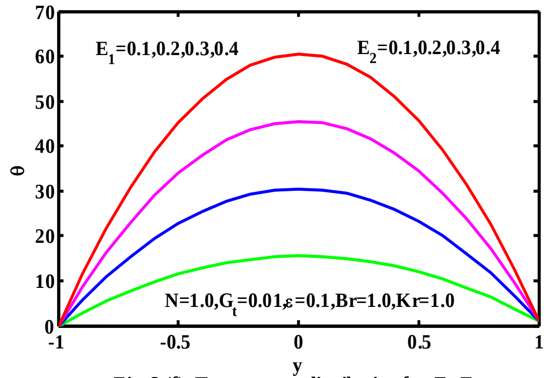

Fig. 2 (f): Temperature distribution for E_1, E_2

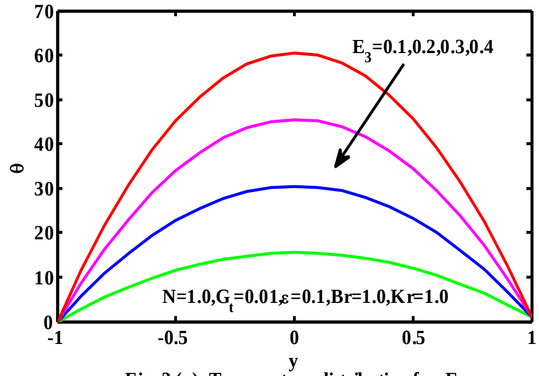

Fig. 2 (g): Temperature distribution for E_3

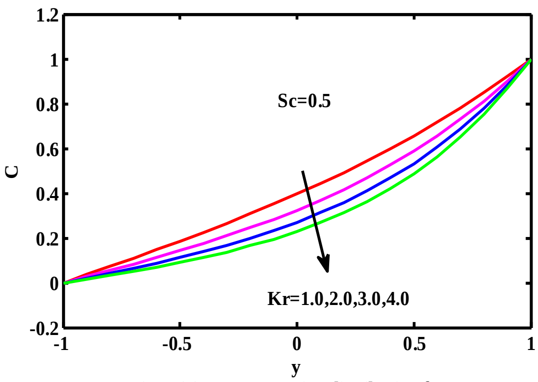

Fig. 3 (a): Concentration distribution for Kr

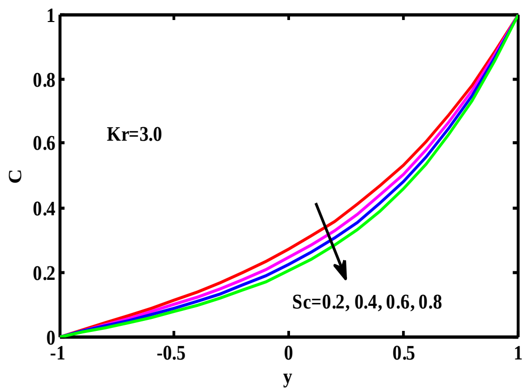

Fig. 3 (b): Concentration distribution for Sc